The Deterministic Description of the Coherent Structure of Free Shear Layers

G. M. Corcos
Department of Mechanical Engineering
University of California, Berkeley

ABSTRACT

The large coherent structures observed in turbulent mixing layers are tentatively identified with the unsteady flow which is generated in two dimensions by the same initial and boundary conditions. This flow is briefly described and means of calculating it are reviewed. Typical results of such calculations are illustrated. For large Reynolds numbers and the outer folds of the interfacial spirals, a boundary-layer-like treatment allows the calculation of the evolution of the diffusive attributes of the flow in terms of the rate of stretching of the material interface. This important quantity has been calculated as a Lagrangian function of time and initial location for a roll-up and pairing and for a moderate Reynolds number. It is suggested that interfacial stretching does not depend strongly on Reynolds number. The use of this convenient approach is illustrated in a simple example of a diffusion-limited reaction.

INTRODUCTION

The mixing layer between two uniform streams is a turbulent flow endowed with a well documented large scale coherent structure. What is most remarkable about this coherent motion is that it appears to be closely similar to the two-dimensional unsteady flow which arises out of the initial superposition of two uniform streams and a few weak two-dimensional perturbations.

We have learned a great deal more about the latter, purely two-dimensional flow that we have been able to measure in a real shear layer so that the evidence and the degree of similarity, while visually striking should perhaps still be viewed as incompletely established.

If, as we believe likely, the coherent structures of turbulent shear layers and the deterministically calculable unsteady flow, which arises in two-dimensions from the juxtaposition of two uniform streams are essentially one and the same, our methods of theoretical study of this turbulent flow should, in our opinion, be revised. In particular:

(a) The deviations from two-dimensionality of a real layer may be viewed as (possibly large) perturbations of the basic two-dimensional time-dependent flow in the sense that their interaction with the flow is evidently unable to destroy or even to control it.

(b) Therefore, such a two-dimensional flow should be used as the base flow for the turbulent mixing layer, no matter how the rest of the flow is calculated, i.e., whether one pursues the deterministic route further by deriving models of three-dimensional motions compatible with and grafted on the time-dependent base flow*, or if one prefers to approximate the three dimensional motion by using plausible functional or phenomenological relations between the known and the unknown parts of the flow. The outstanding simplification is that the base flow which is proposed as a substitute for the usual mean flow has an independent existence.

In this short survey, we will focus on the description of the two-dimensional unsteady flow, and in particular, we shall evaluate available methods of computing it, give examples of these configurations, suggest methods of generalizing them, and discuss a few applications. For a more comprhensive discussion these and other aspects of the problem, Patnaik, Sherman and Corcos (1976), Corcos and Sherman (1976) and Corcos (1979) may be consulted.

A Thumb-nail Sketch

As is now well known, a two-dimensional shear layer rolls up in a connected row of spirals whose spacing and diameter grow with streamwise distance from the origin. The first spirals are the result of the shear layer instability whose origin is described by linear theory. But, while this first instability is self-limiting,

*For a progress report on such an approach, see Corcos (1979). A substantial amount of additional work in this area is being carried out at Berkeley.

the configuration is unstable to subharmonic perturbations and the spirals pair or amalgamate and, as a result, both the circulation around a spiral and the spacing between two adjacent spirals increases.

As the original interface is distorted into a spiral, it is stretched on the average because its total length steadily increases. As a result, the region to which the original spanwise vorticity of the layer is confined thins out and the volume occupied by the vorticity at any time is a fraction of the volume of the fluid which appears to be sheared (the space within the nominal outline of the shear layer).

The focii of the spirals are points of accumulation of spanwise vorticity. Between them, there are stagnation points which are saddles, the neighborhood of which is depleted of spanwise vorticity. They are the site of intense deformation, consistently positive in the direction of the interface.

As we shall see, around the focii of the spirals, the successive coils become not only dense, but also wide, because they suffer compression, and they form a solid core in which vorticity gradients and gradients of diffusive attributes of the layer are in general far more gradual.

We have mentioned that coils of vorticity coalesce. According to both computations and to observations, the preferred mode involves two coils at a time. When two coils pair, the saddle which was in between (an irrotational stagnation point) is destroyed. But it survives long enough to contribute, during the pairing and for a certain time afterwards, an intense strain in between the two vortex centers. This strain in turn causes energetic interdiffusion of vorticity between the two previously separated vortex centers. Nevertheless the pairing vortices while pressed against one another retain a separate identity for a substantial time after pairing so that a stationary probe, past which paired vortices are convected would be likely to detect a large oscillation in velocity near the apparent center of the new vortex.

Computation of the Flow

By now, a number of independent numerical simulations of the two-dimensional shear layer have been carried out, by Ashurst (1977), Patnaik, Sherman and Corcos (1976), Peltier, Halle and Clark (1978), Delcourt and Brown (1979) and others. They include simulation of the vorticity distribution by a large number of point vortices and simulation of the Navier-Stokes equation by finite differences.

While all these simulations are very suggestive of the coherent structures observed in the laboratory, the finite differences solutions of the diffusive equations for the temporally developing instability and for moderate Reynolds numbers has been carried out in greatest detail. Its main drawback is that practical flows develop streamwise rather than temporally, and that a mapping only gives an approximation to the former in terms of the latter.

I shall only discuss temporal simulation by finite differences, with which our group has had substantial experience.

In these computations, the flow develops in time on a grid in which the streamwise boundary conditions are periodic. The initial flow is the superposition of a simple shear layer and one or several eigenfunctions of the linear stability problem. One of the eigenfunctions corresponds in general to the wave number of the fastest growing wave according to linear theory, since that wave is known to dominate the early instability in a natural flow. The other eigenfunctions correspond to subharmonics of that wave.

While the cyclical boundary conditions limit the number of subharmonics which can be studied simultaneously with the fundamental with good resolution, the solution for the simultaneous growth of a fundamental and two subharmonics (wave length ratios 1, 2, 4) is currently carried out at reasonable cost.

Resolution limits the maximum value of the Reynolds number. We are routinely using an initial Reynolds number $U\delta/\nu = 100$, where

$$\delta = \frac{\Delta U}{2(\partial U/\partial z)_{max.}} \qquad \text{and} \qquad U = \Delta U/2$$

Our computations provide as printed outputs many details of the flow such as the two components of velocity, the vorticity and the pressure at all grid points, the integral of the Reynolds stress, the rate of dissipation, the momentum thickness, the maximum elevation of the limiting closed streamline (cat's eye), the area enclosed by that streamline, the rate of increase of the fluctuation kinetic energy. Plots are provided at regular intervals of streamlines, and constant vorticity contours. Other quantities of dynamic importance are also calculated as a by-product of the computation. Some of these will be discussed later.

As an illustration, figures (1 abcd) reproduce plots of vorticity contours and of selected streamlines during the later stages of a first pairing between fundamental and its first subharmonic and figures (2 abcd) show similar plots for an initial condition which includes fundamental, first and second harmonic perturbations. For the latter case, the times chosen on the figure corresponds to the second pairing.

It is, of course, also possible to compute the evolution of a passive scalar which diffuses from one steam to the other (e.g., temperature, if one stream is slightly warmer than the other). This is illustrated in Figure (3 ab).

Development in time vs. streamwise development

Can our time-developing layers be used to model streamwise development?

There is no reason of course why a mapping of one onto the other should satisfy the governing equations precisely. It is known for instance that the initial infinitesimal growing waves are non-dispersive for the instability in time of x-wise periodic waves, while they are weakly dispersive for the streamwise instability of time-wise periodic waves.

Nevertheless, such a mapping may be useful for many approximate purposes. For instance, one may postulate that if x, z, t are coordinates and time in the temporal problem x', z', t', the corresponding coordinates and time in the streamwise case, $\overline{U}$, the average velocity of two streams, and ω is the spanwise vorticity,

$$\omega(x, z, t) = \omega'(x', z', t')$$

where

$$z' = z \qquad z = z'$$

$$x' = \overline{U}t \qquad x = x' - \overline{U}t'$$

$$t' = t - x/\overline{U} \qquad t = x'/\overline{U}$$

The vorticity equation expressed in the coordinates of the streamwise problem is

$$(2 - u'/\overline{U})\frac{\partial\omega'}{\partial t'} + \overline{U}\frac{\partial\omega'}{\partial x'} + w'\frac{\partial\omega'}{\partial z'} = \nu\left\{\frac{1}{\overline{U}^2}\frac{\partial^2\omega'}{\partial t'^2} + \frac{\partial^2\omega}{\partial z'^2}\right\}$$

This equation is clearly wrong, but it indicates that the accuracy of the mapping increases as $\overline{U}/\Delta U$ increases. A measure of the error of the mapping is the difference at any point between the velocity V associated with ω in the temporal calculation and the velocity V' induced by the distribution $\omega' = \omega$ at any corresponding point x'*. We are presently making such a comparison in connection with the question: What role do the paired downstream vortices have in exciting subharmonic perturbations upstream, i.e. is there a strong feedback?

For other purposes, a grid computation with boundary conditions relevent to a streamwise-growing-layer is indicated. The main difficulty with this version of the problem is that while it is elliptic, the downstream boundary condition is unknown. However several variations of a scheme which neglects streamwise diffusion over the last streamwise interval can be derived and the distribution of vorticity which would be found downstream of the grid can be idealized with varying degrees of realism, e.g. by use of the transformation suggested above.

Such a computation would be particularly valuable for the study of the early nonlinear period of development. For instance, it might well shed welcome light on the nature of the competitive growth of two periodic perturbations of the layer slightly different (incommensurate) in frequency around the frequency for maximum initial growth rate.

Extension to large Reynolds numbers

It is clear that where the coils are thin and distinct, the dominant gradients of vorticity, concentration, etc. are normal to the coil and further, that the shear across a coil has only a minor effect on diffusion across it. Thus, for computation

*This suggests that the mapping is the first term of an expansion of the streamwise-developing vorticity in powers of $\varepsilon = \Delta U/U$.

of the flow quantities in the neighborhood of a coil, an adequate approximation to the advective operator is

$$\frac{\partial}{\partial t} + \vec{u} \cdot \nabla \cong \left(\frac{\partial}{\partial t}\right)_{\vec{s}o} - \gamma\,(\vec{s}o,t)\,\eta\,\frac{\partial}{\partial \eta} \qquad (1)$$

where the time derivative on the right is taken as Lagrangian (s_o is the location of a material point at the original interface), V_s is the velocity along the material interface whose local direction is $\vec{s}$, s is the local coordinate along this interface and η a coordinate normal to s. This Lagrangian operator casts advective problems as local problems solved along the characteristic $s = so + \int V_s\, dt$. The approximations leading to eqn (1) require not only a high Reynolds number, but also a sufficiently positive value of the Lagrangian integral $\int_o^t \gamma(t',so)dt'$, in order that diffusive layers be narrow and centered on the material interface. Its use requires the knowledge at all times both of the location of identified points of the material interface and of the Lagrangian function $\gamma(s_o, \tau)$, the interfacial strain rate which is also the logarithmic extension rate of an interfacial segment.

From numerical calculations for several Reynolds numbers and somewhat weaker (i.e., less direct) experimental evidence, we suggest that the material interface location and the function γ are both only weakly affected by the Reynolds number* and we propose that their values computed at a Reynolds number = 100 as part of our finite difference solutions can reasonably be used for all Reynolds numbers.

The Interfacial Evolution

Figures 4 give an idea of the computed evolution of interfacial markers for a simple roll-up and figures 5 for a roll-up and a first pairing. Figures 6 and 7 show the corresponding Lagrangian functions $\gamma(so, \tau)$ for the two cases.

The results indicate that while on the average, the length of the material interface increases substantially (by a factor close to 4 for a roll-up from $\tau = \frac{tU}{\lambda\sigma} = 0$ to $\tau = 2.0$; by a factor of about 8 for a roll-up and pairing from $\tau = 0$ to $\tau = 2.50$), the Lagrangian strain function γ is anything but monotonic with either s_o or time. The total strain of individual elements of the interface vary with initial location by a factor of about 130 in the first case and by more than 500 in the second. Some sections of the initial interface are more consistently compressed than stretched and therefore any diffusive thickness associated with such segments would increase at any Reynolds number rather than decrease. In general, a sample solution of an interfacial diffusion problem of the type

$$\frac{\partial c}{\partial t} - \gamma \frac{\partial c}{\partial \eta}\,\eta = D\,\frac{\partial^2 c}{\partial \eta^2}$$

---

*This is less true for the initial roll-up than for subsequent pairings.

yields a diffusive layer thickness, $\delta(s_o, t)$ which, for a given value of t, increases almost monotonically from the saddle (the middle of the braid) to the focus in a roll-up; a substantial part of the region surrounding the focus in the core would be occupied by overlapping rather than distinct diffusive layers at any Reynolds number. During pairing, the behavior of γ is still more complex. In particular, the region along the interface midway between two merging vortex cores is subject to an especially large positive strain which enhances the inter-diffusion of the two vortex centers. We have not yet analyzed these recent results carefully. But it already seems clear that the boundary layer-type approximations which we have mentioned for high Reynolds numbers are only applicable to the braids and to the external folds of the spiral. On the other hand, for many applications in which total rate of mixing or rate of diffusion-limited reaction is desired, these are the regions which make by far the greatest contribution to these rates.

An application: Diffusion-limited reaction

The knowledge of the interfacial properties of the shear layer can readily be used in problems involving diffusion and chemical reactions between the two streams. We use a simple example as an illustration. It is an extension of that offered by Marble and Broadwell (1977).

The two streams have different chemical compositions and can react with each other. The binary reaction is fast enough to be diffusion-limited. Let K_1, K_2 be the mass fraction of the two reacting species, K_3 that of the product. All three satisfy the equation

$$\frac{\partial K_i}{\partial t} - \gamma z \frac{\partial K_i}{\partial z} = D_i \frac{\partial^2 K_i}{\partial z^2} \tag{2}$$

under the conditions discussed earlier. Assume $D_i = D$ for all three species. Neglect the effect which the reaction may have on the motion. The diffusion layers are assumed distinct from one coil to the other so that K_1 and K_2 reach asymptotic values away from the reaction surface. Let z_o (T, s_o) be the normal distance of the reaction surface from the material interface. If f is the stoichiometric ratio, Marble and Broadwell (1977) show that

$$\frac{\partial K_1}{\partial z}(zo, t) \Big/ \frac{\partial K_2}{\partial z}(zo, t) = - f \tag{3}$$

K_1 is found for $z > z_o$, K_2 for $z < z_o$ and, at $z = z_o$, $K_1 = K_2 = 0$. K_3 is produced at the reaction surface and is found on either side of it. Mass conservation gives at the surface the equation

$$\left(\frac{\partial K_1}{\partial z} + \frac{\partial K_3}{\partial z}\right)_{z = z_o^+} - \left(\frac{\partial K_2}{\partial z} + \frac{\partial K_3}{\partial z}\right)_{z = zo^-} = 0 \tag{4}$$

at $z = z_o$, the fluid normal velocityis due to the net mass flow across the surface, i.e.:

$$D\left(\frac{\partial K_1}{\partial z} + \frac{\partial K_3}{\partial z}\right)_{z = zo^+} = - \rho w\ (z_o)$$

Now, take the reaction surface as the origin, $y = 0$ and assume the similarity form

$$K_i = f_i \left(y/\delta_D\ (s_o,t)\right) = f_i\ (\eta)$$

with boundary conditions

$$\begin{pmatrix} K_1 \\ K_2 \end{pmatrix} = 0 \quad \text{for } y = 0; \qquad \begin{aligned} K_1 &\to K_{1\infty}, \quad \eta \to \infty \\ K_2 &\to K_{2\infty}, \quad \eta \to -\infty \end{aligned}$$

then one finds that

$$K_1 = \frac{K_{1\infty}}{1-\alpha}\left[\text{erf}\left(\frac{\pi^{1/2}}{2}\ \eta + \beta/\pi^{1/2}\right) - \alpha\right] \tag{5a}$$

$$K_2 = \frac{K_{2\infty}}{1+\alpha}\left[\text{erf} -\left(\frac{\pi^{1/2}}{2}\ \eta + \beta/\pi^{1/2}\right) + \alpha\right] \tag{5b}$$

Where $\alpha = \text{erf}\ \beta/\pi^{1/2}$; equation (3) leads to

$$\alpha = \frac{1-\phi}{1+\phi}$$

where ϕ is the equivalence ratio,

$$\phi \equiv \frac{K_{1\infty}}{K_{2\infty} f} \tag{6}$$

The local volume consumption rates are

$$V_1 = D\left.\frac{\partial K_1}{\partial y}\right|_{y = o} = \frac{K_{1\infty} D}{\delta_D}\ \frac{\phi+1}{2\phi}\ e^{-\beta^2/\pi} \tag{7a}$$

$$V_2 = -D\left.\frac{\partial K_2}{\partial y}\right|_{y = o} = \frac{K_{2\infty} D}{\delta_D}\ \frac{\phi+1}{2}\ e^{-\beta^2/\pi} \tag{7b}$$

where:

$$\delta_D^2 = \delta_D^2\,(t = o,\ s_o)\ \exp.\left[-\int_o^t 2\gamma dt'\right] + \pi D \int_o^t \exp.\left(-\int_{t'}^t 2\gamma dt''\right)\ dt' \qquad (8)$$

The total reactant consumption up to time t is found by integrating first in time for an identified segment of the reaction interface and then over the whole initial reaction surface. For reactant 1, this is for instance,

$$C_1 = D\,K_{1\infty}\ \frac{\phi+1}{2\phi}\ e^{-\beta^2/\pi} \int_o^{\lambda o}\left[\int_o^t \left(\frac{1}{\delta_D(so,t')}\int_o^{t'} \exp\ \gamma\ dt''\right) dt'\right] ds_o \qquad (9)$$

where λ_o is the initial length of the reaction surface considered. δ_o is given by equation (7) and γ by the computation discussed earlier.

The rate of generation of product (3) is the sum $V_1 + V_2$ and one finds easily that

$$K_3 = K_{30}\left(1 - \frac{K_1}{K_{1\infty}}\right);\qquad y > 0 \qquad (10a)$$

$$K_3 = K_{30}\left(1 - \frac{K_2}{K_{1\infty}}\right);\qquad y < 0 \qquad (10b)$$

where $K_{30} = K_3(y = 0) = K_{2\infty}\,(f + 1)\ \frac{1+\alpha}{2}$.

We note, from the form of eqs. (8) and (9) that production takes place almost exclusively where $\int_o^\tau \gamma\ d\tau > 0$, so that the solid cores where the treatment above is inappropriate because $\int_o^\tau \gamma d\tau < 0$ there in general, makes only minimal contributions to the production; on the other hand the products should occupy the core almost exclusively. For a real turbulent shear layer, it would seem realistic to expect the stochastic nature of the large scale (i.e. two-dimensional) structures to have little effect on the reaction rate. On the other hand the small, three-dimensional scales which are observed to grow rapidly and to create a mixing transition (Konrad, 1977, Breidenthal, 1978), need to be taken into account. One should replace the molecular diffusion coeeficient D, by a local eddy-diffusivity related to γ and to its Lagrangian history. At this time we have little experimental data and insufficient theoretical models to define this relation.

A speculation about the origin of the randomness of the coherent structures in the shear layer

As was demonstrated by Brown and Roshko (1974), the coherent structures which occur in an experimental shear layer evolve with a substantial measure of randomness. Thus at a fixed point, the frequency of passage of vortex cores is broadly distributed

around a mean, the location of the n^{th} pairing fluctuates etc. Yet the model which we have offered for these structures is fully deterministic. The difference can conceivably come from two distinct sources. The first one is that in the calculation we control the phase, wave length and amplitude of all initial disturbances (fundamental and subharmonics) while the background fluctuations upon which the sequential instabilities feed in a natural flow are evidently random. The second possible cause, which is more or less axiomatic in usual discussions of turbulence is that the flow is effectively not unique in the sense that an infinitesimal perturbation in, say, the boundary conditions leads rapidly to a finite variation in the flow field. The difference is subtle but real, since in the first case a proper, say, statistical, definition of the initial conditons may lead via stable solutions, to an accurate statistical description of the solution, while in the second, there is no obvious way to construct the statistics. We suggest that a flow in which the only sequential instabilities are subharmonic is unlikely to be sensitive to small perturbations during its finite development and is in fact neutrally stable to such influences. In principle, then, we suggest that the random properties of the coherent structures may be calculable from the statistics of the initial perturbations. We have as yet no evidence to support this suggestion except the insensitivity of our numerical calculations to small round-off errors.

F.S. Sherman and S.Y. Lin have both considerately contributed to the calcualtions discussed above.

References

Ashurst, W.T. (1977) Numerical Simulation of Turbulent Mixing Layers via Vortex Dynamics. SANDIA Laboratories Report SAND 77-8613.

Breindenthal, R.E. (1978) A Chemically Reacting Shear Layer. Thesis, Cal. Inst. Tech.

Brown, G.L. and Roshko, A. (1974) On Density Effects and Large Structure in Turbulent Mixing Layers. J. Fluid Mech. 64, 775.

Corcos, G.M. (1979) The Mixing Layer: Deterministic Models of a Turbulent Flow. University of California, Berkeley, College of Eng. Report No. F. M-79-2.

Corcos, G.M. and Sherman, F.S. (1976) Vorticity Concentration and the Dynamics of Unstable Free Shear Layers. J. Fluid Mech. 73, 241.

Delacourt, B.A. and Brown, G.L. (1979) The Evolution and Emerging Structure of a Vortex Sheet in an Inviscid and Viscous Fluid Modelled by a Point Vortex Method. Second Symposium on Turbulent Shear Flows, July 2-4, 1979, Imperial College, London, England.

Konrad, J.H. (1977) An experimental Investigation in Two-Dimensional Turbulent Shears Flows with Applications to Diffusion-Limited Chemical Reactions. Thesis, Calif. Inst. Tech.

Marble, F.E. and Broadwell, J.E. (1977) The Coherent Flame Model for Turbulent Chemical Reactions. Project SQUID Report, Contract No. 4165-52 and 8960-18.

Patnaik, P.C., Sherman F.S. and Corcos, G.M. (1976) A Numerical Simulation of Kelvin-Helmholtz Waves of Finite Amplitude. J. Fluid Mech. 73, 215.

Peltier, W.R., Halle, J. and Clark, T.L. (1978) The Evolution of Finite Amplitude Kelvin-Helmholtz Bellows. Geophys. and Astrophys. Fluid Dyn. 10, 53.

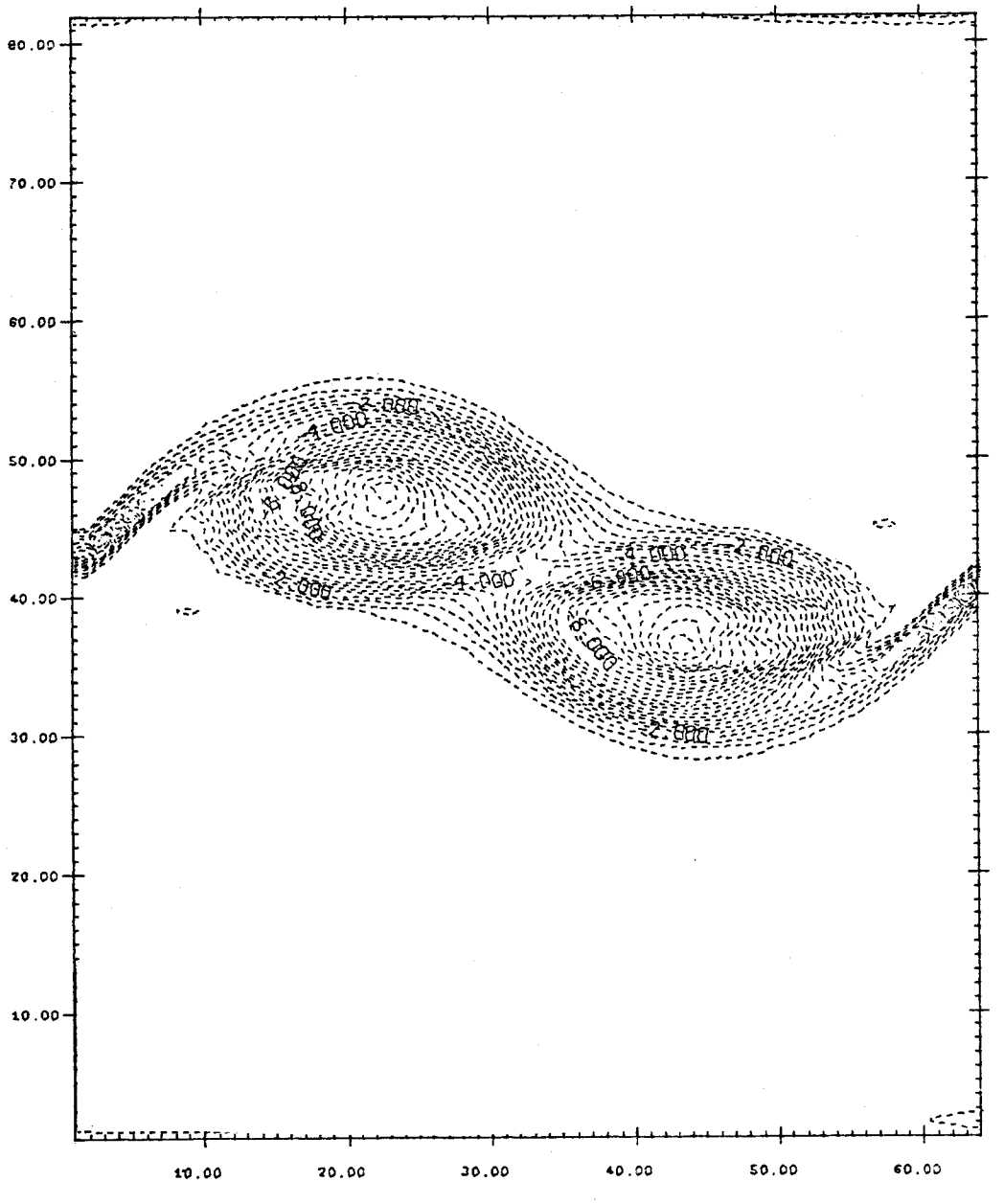

Fig. 1a Vorticity contours. Roll-up and pairing. $\alpha_1 = 0.43$; $\alpha_2 = 0.215$; $R_e = 100.$

$\tau = \frac{tU\alpha}{2\pi\delta} = 2.$ Ω max ≈ 13.5

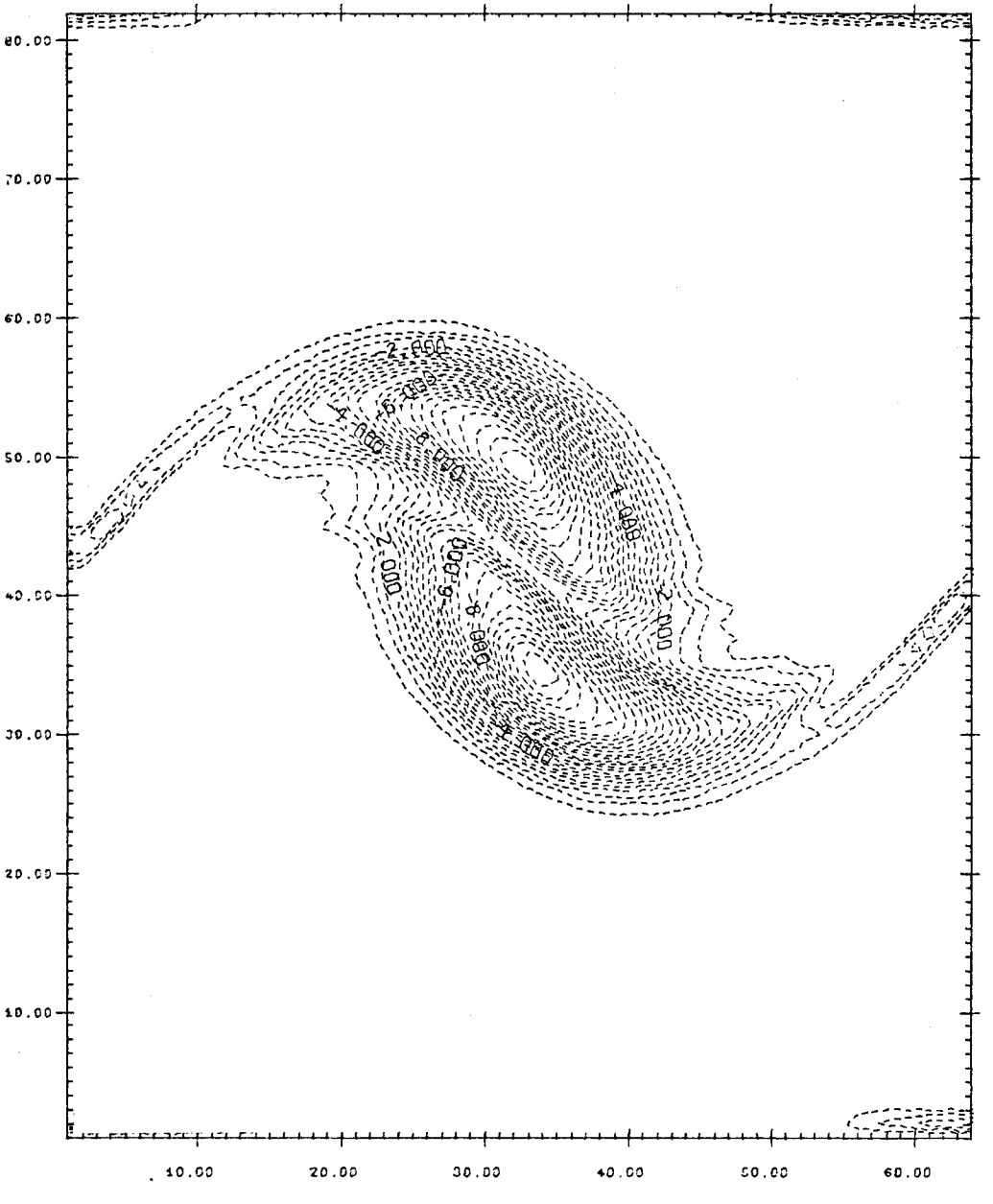

Fig. 1b Vorticity contours. Same case as 1a. $\tau = 2.5$

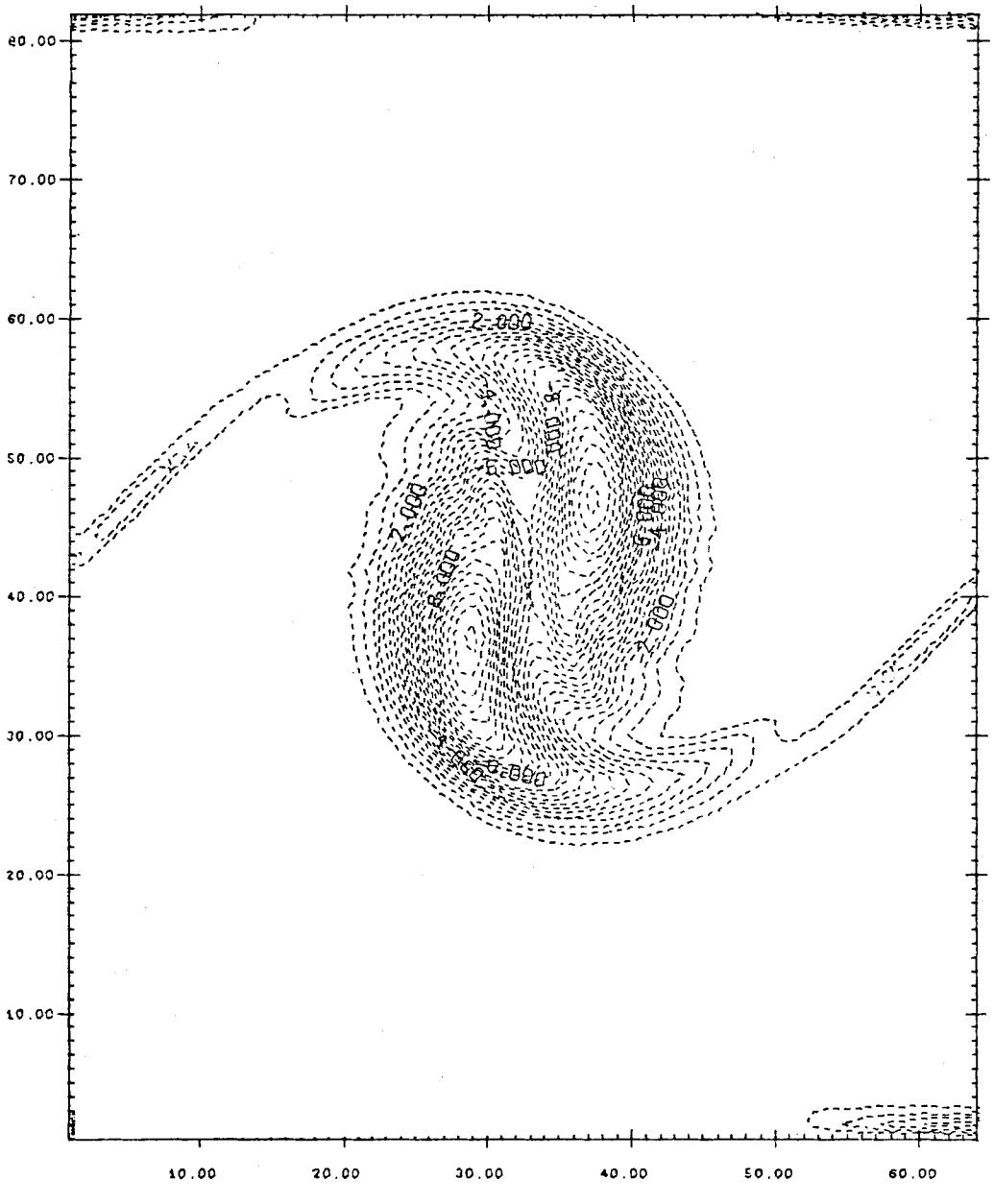

Fig. 1c Vorticity contours. Same case as 1a. $\tau = 2.75$

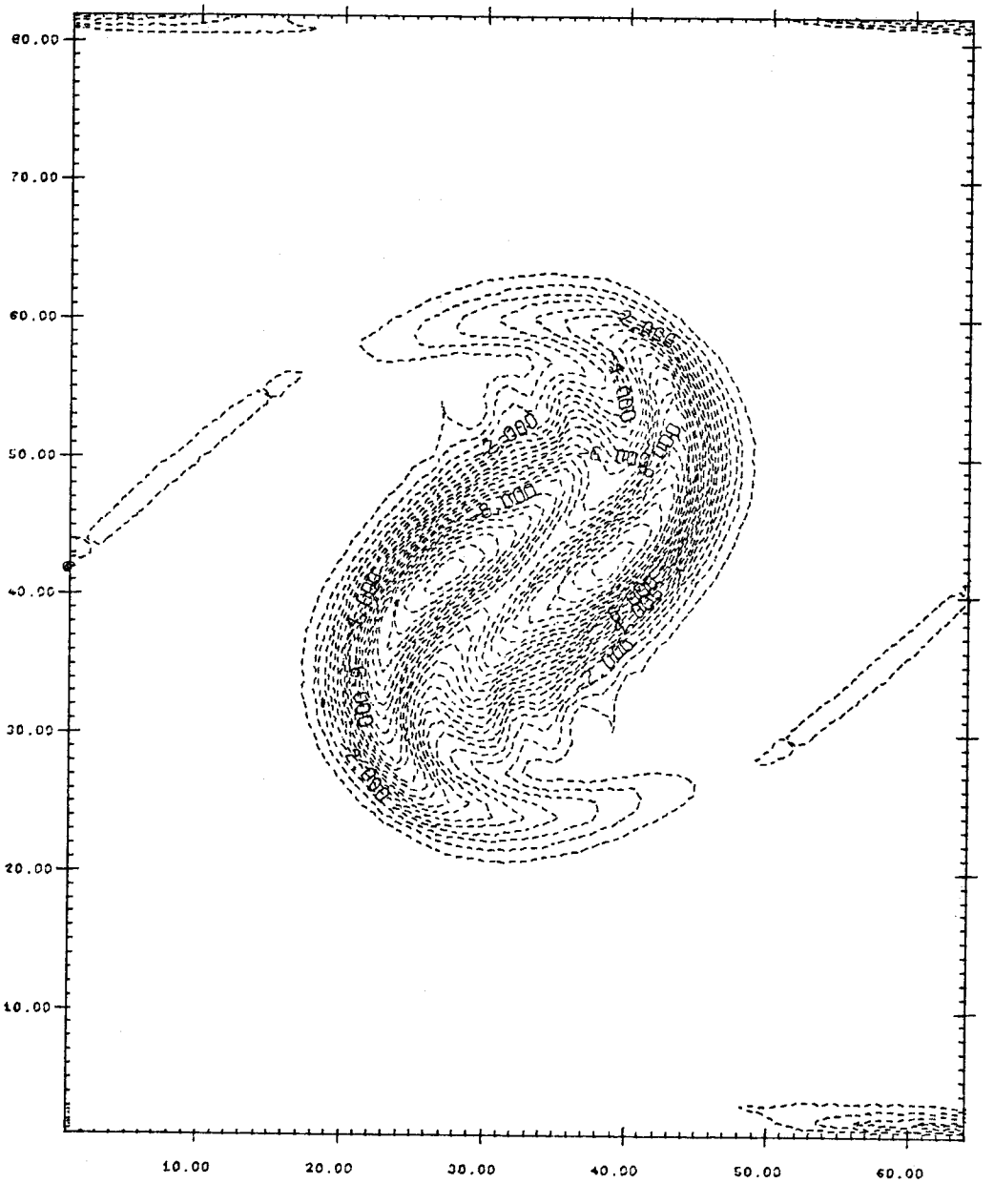

Fig. 1d Vorticity contours. Same case as 1a. $\tau = 3.0$

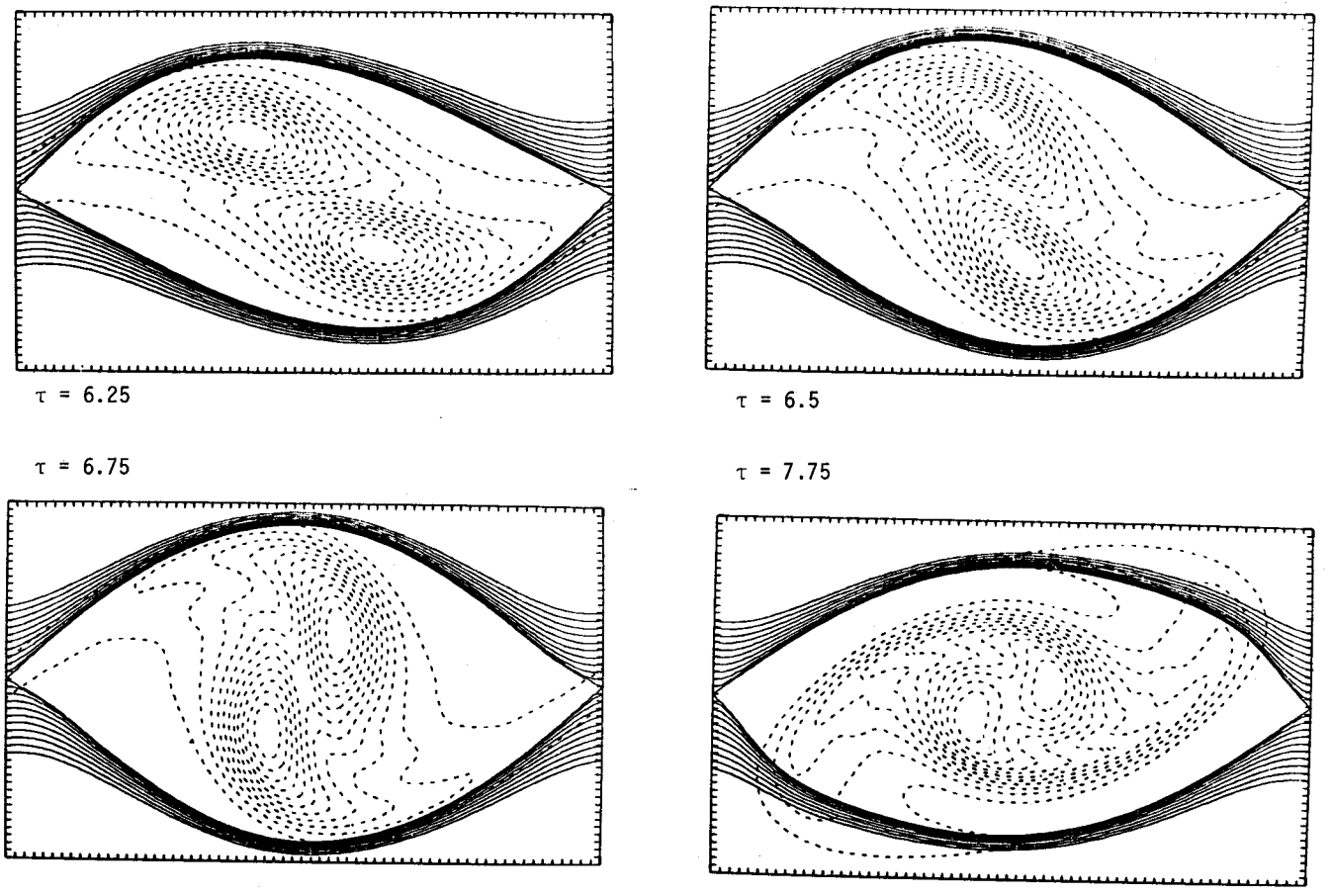

Fig. 2 Vorticity Contours (---) and streamlines (——). Roll-up and two successive pairings. $\alpha_1 = 0.43$. $\alpha_2 = 0.215$; $\alpha_3 = 0.1075$; $R_e = 50$. The first pairing has left no trace of the shorter wave.

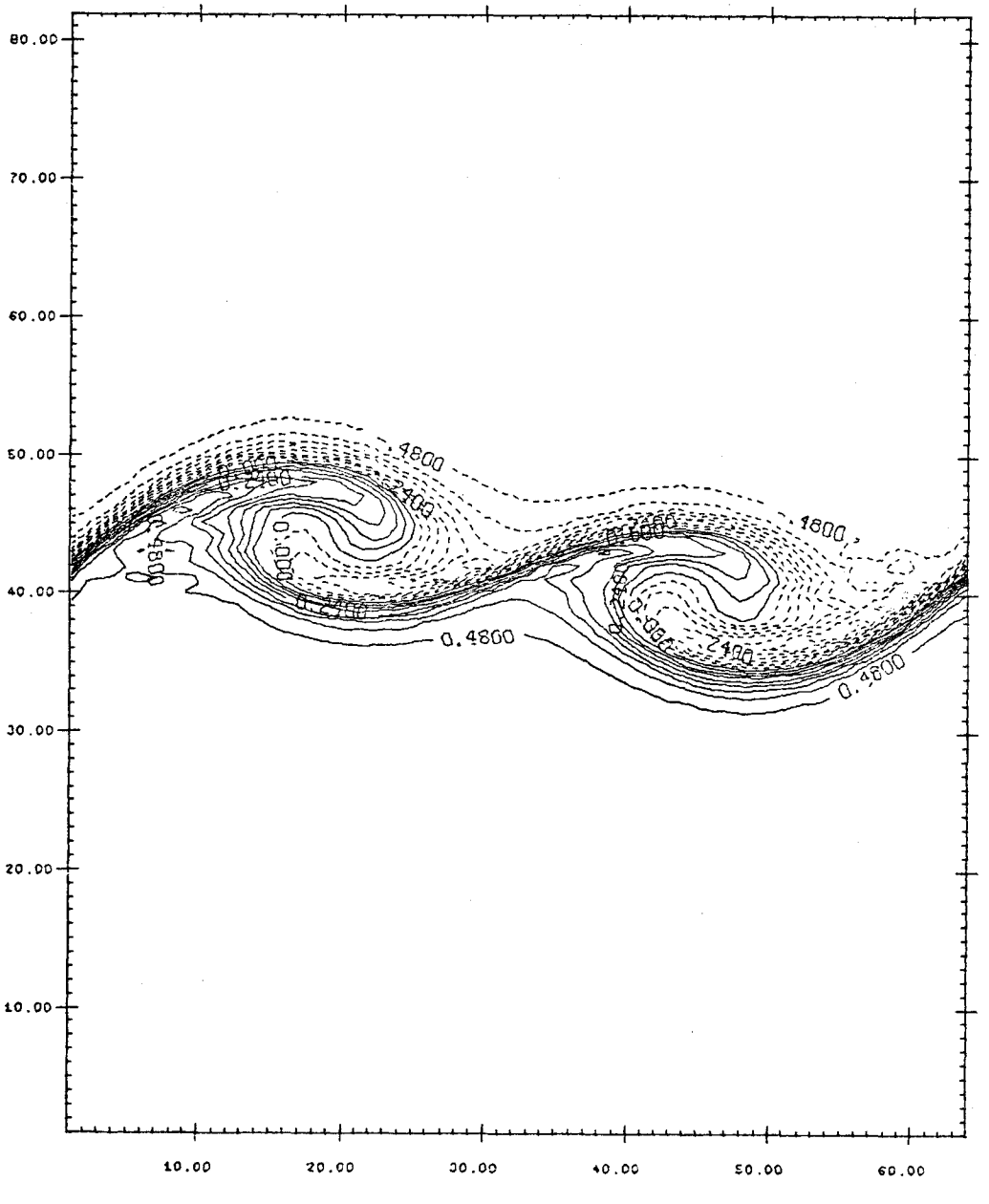

Fig. 3a Diffusion of a passive scalar. Pr = 0.72. Lines of constant concentration. Same case as labcd. Free stream values of scalar {± 0.500. τ = 1.50

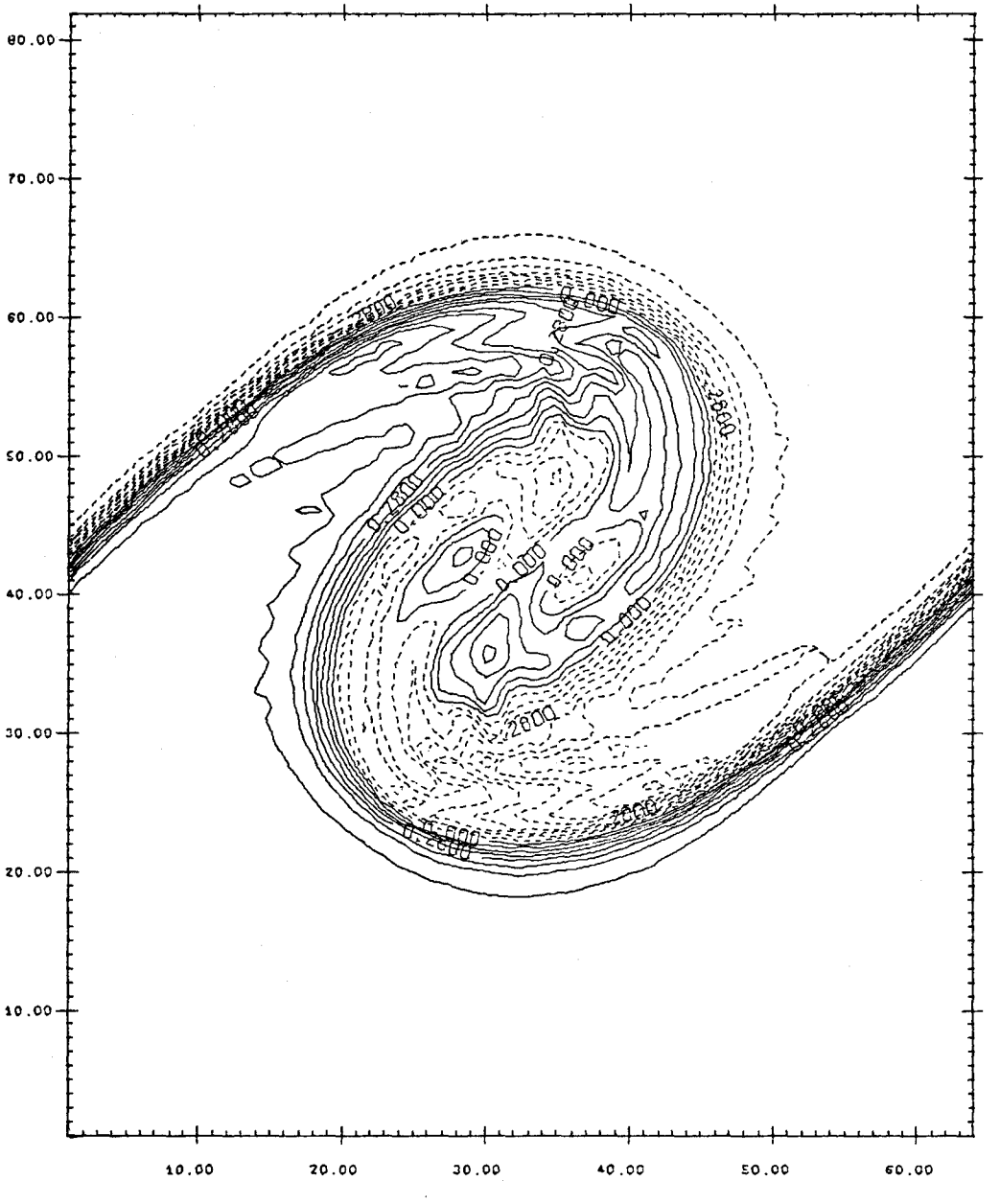

Fig. 3b Same case as 3a. τ = 3.00

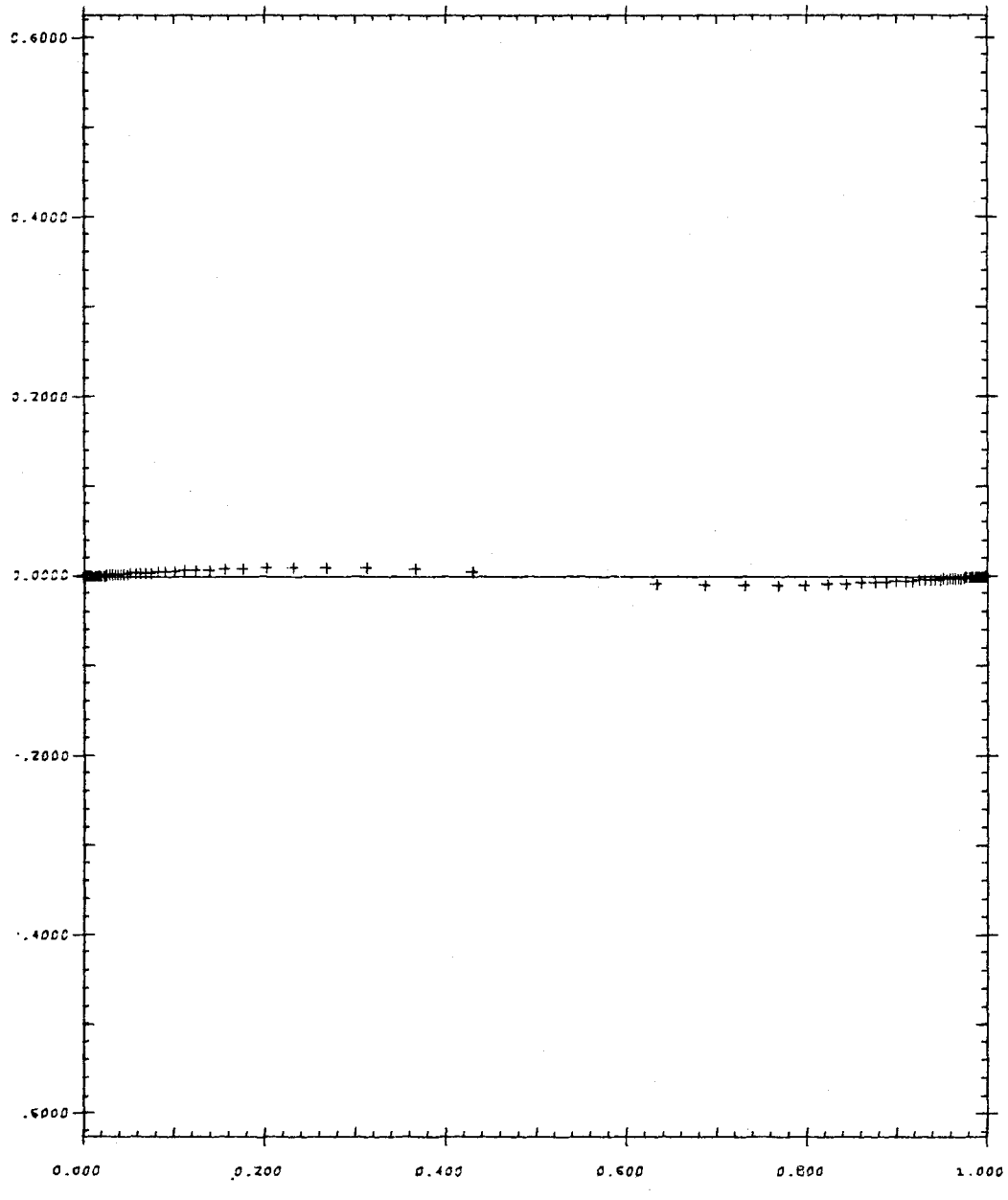

Fig. 4a The evolution of the material interface. Crosses are non-diffusive markers. Roll-up; $\alpha = 0.43$. $R_e = 100$ $\tau = 0$

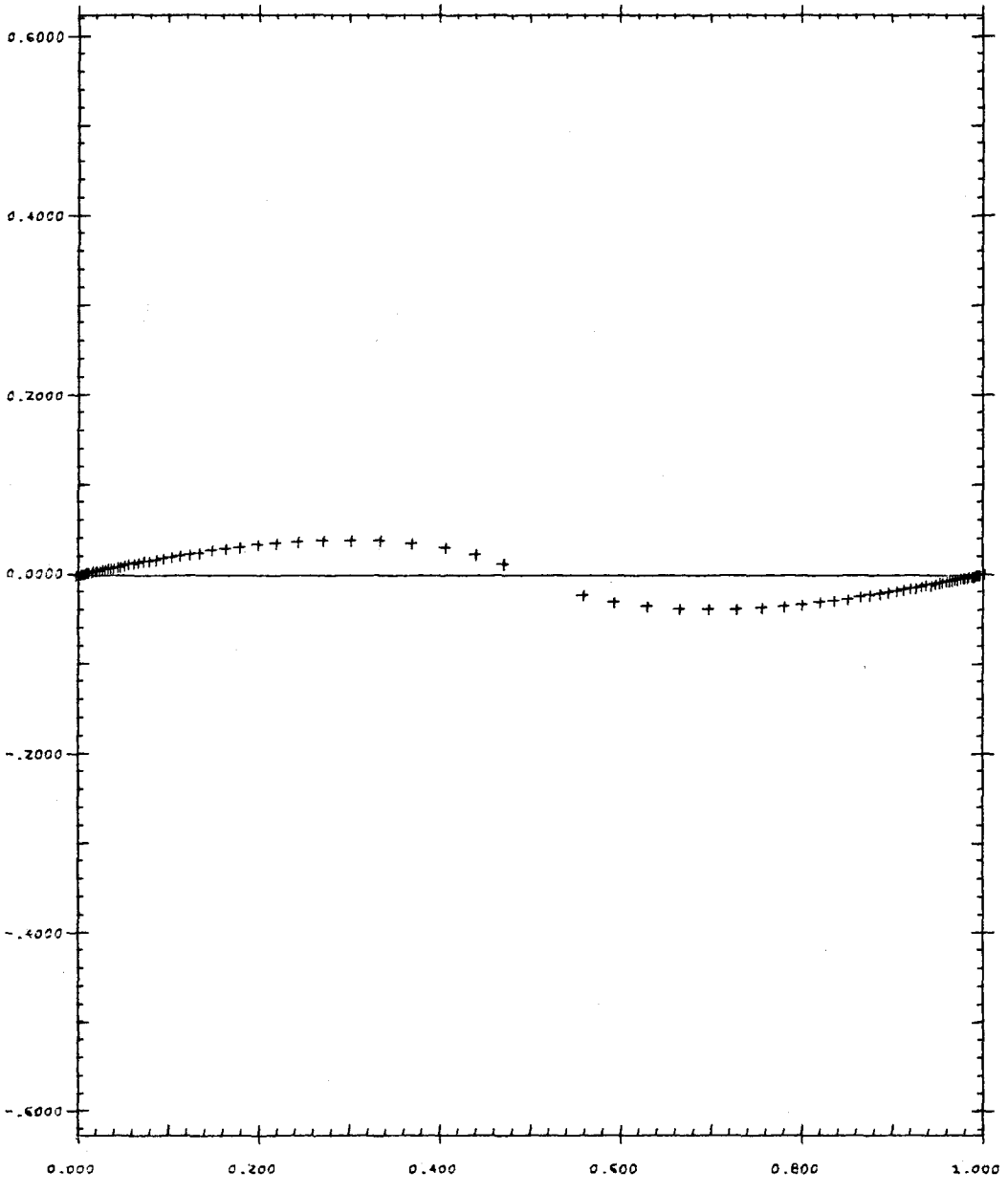

Fig. 4b Same as 4a; $\tau = 0.50$

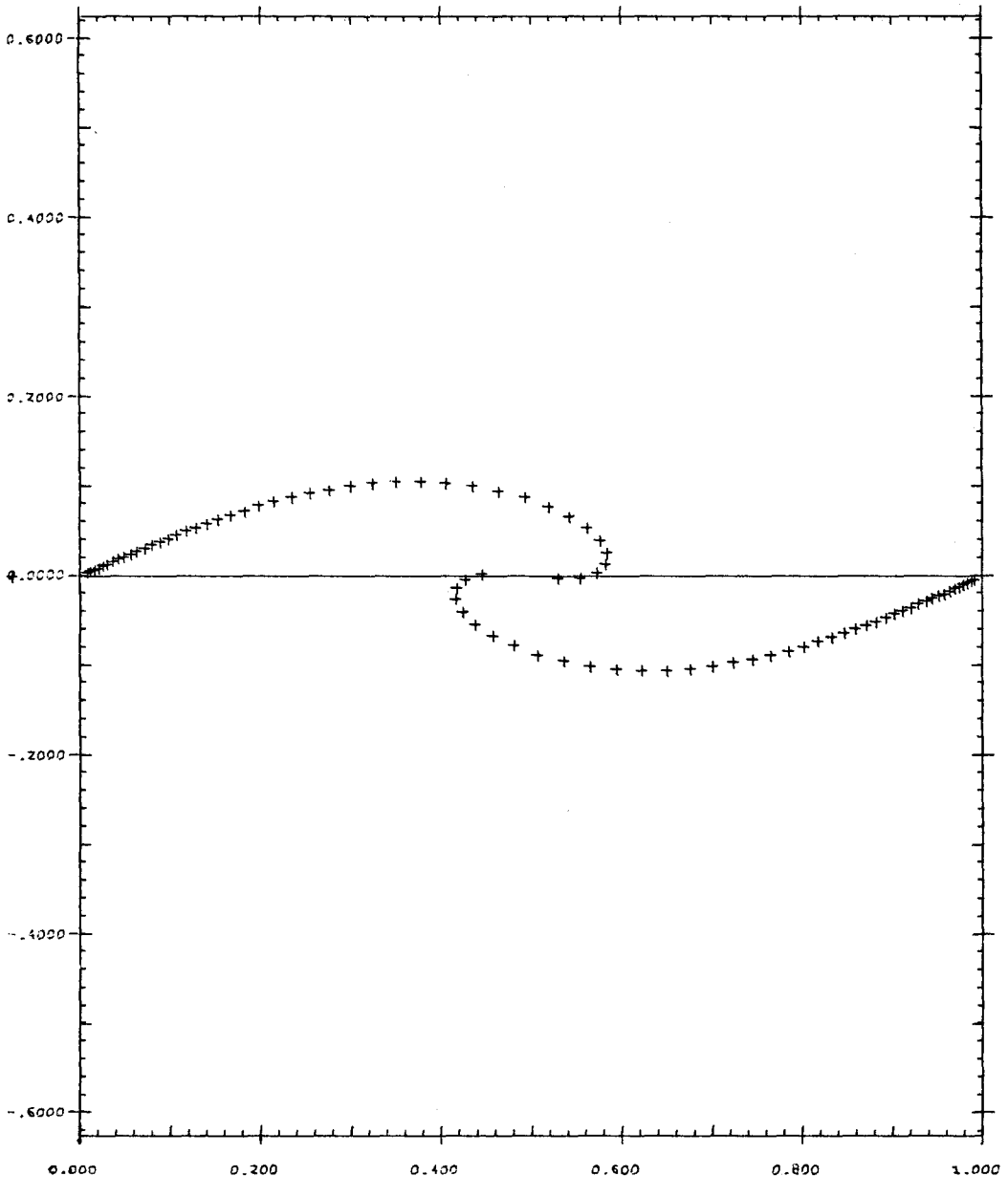

Fig. 4c Same as 4a; $\tau = 1.0$

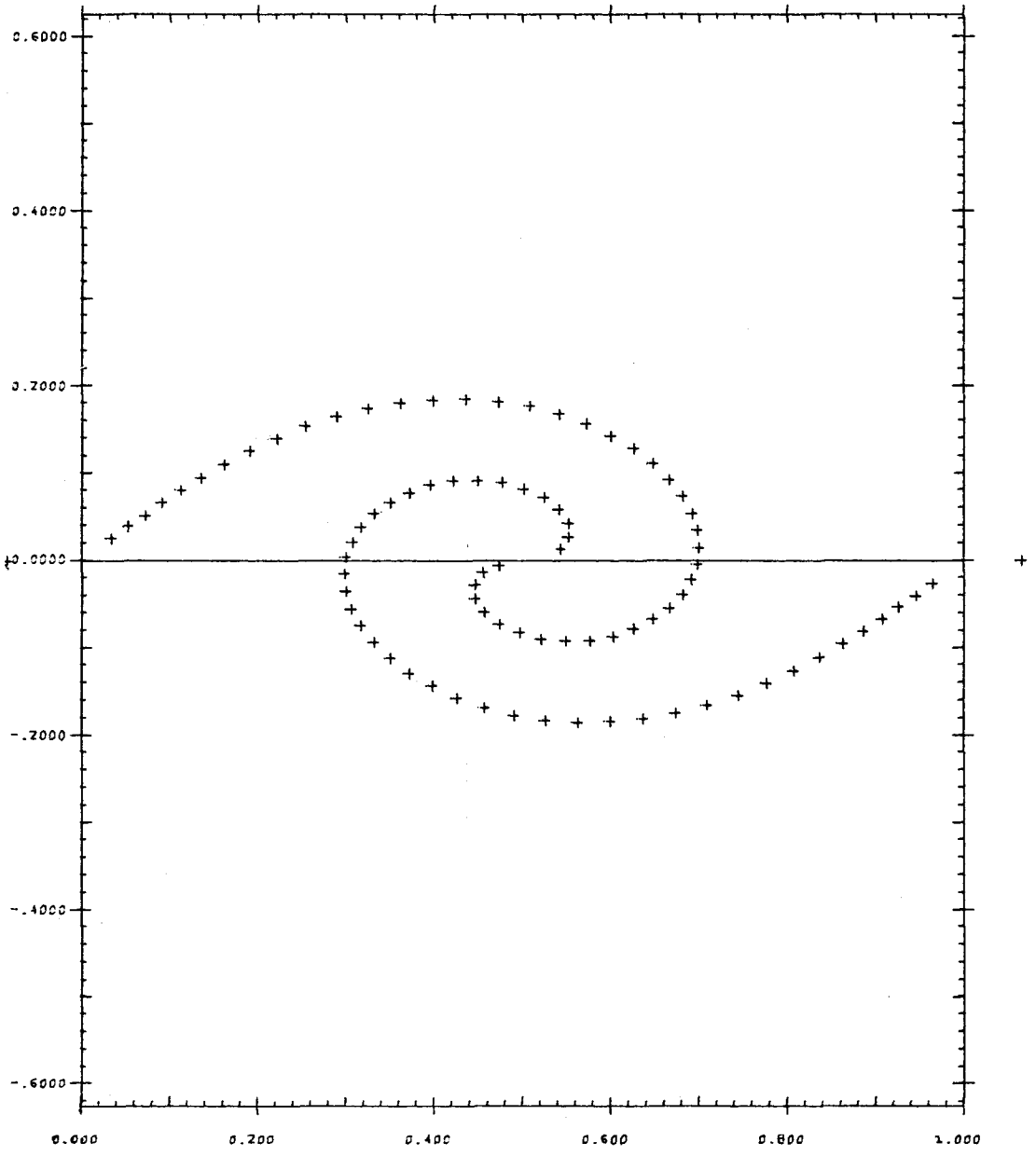

Fig. 4d Same as 4a; $\tau = 1.50$

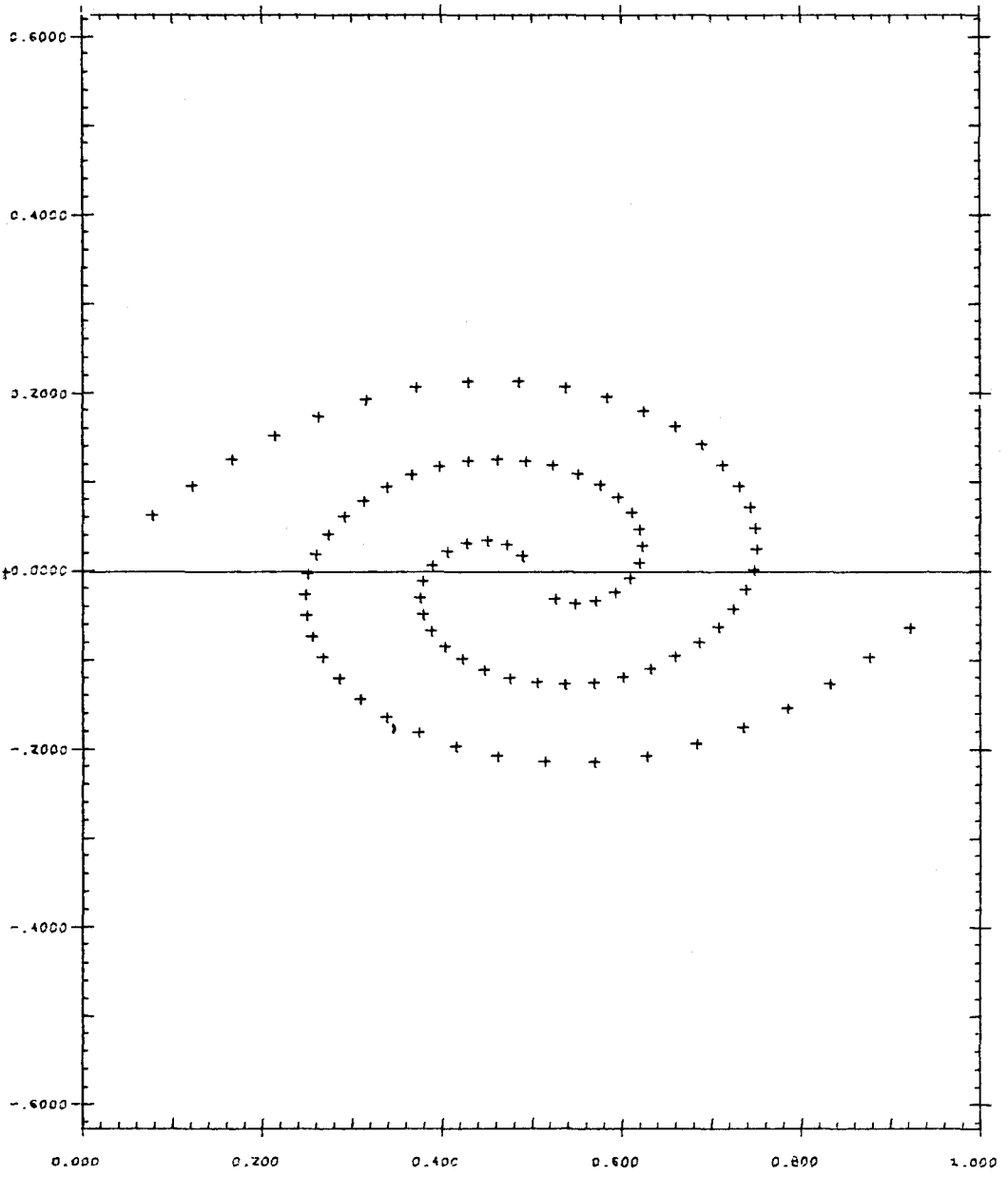

Fig. 4e Same as 4a; $\tau = 1.75$

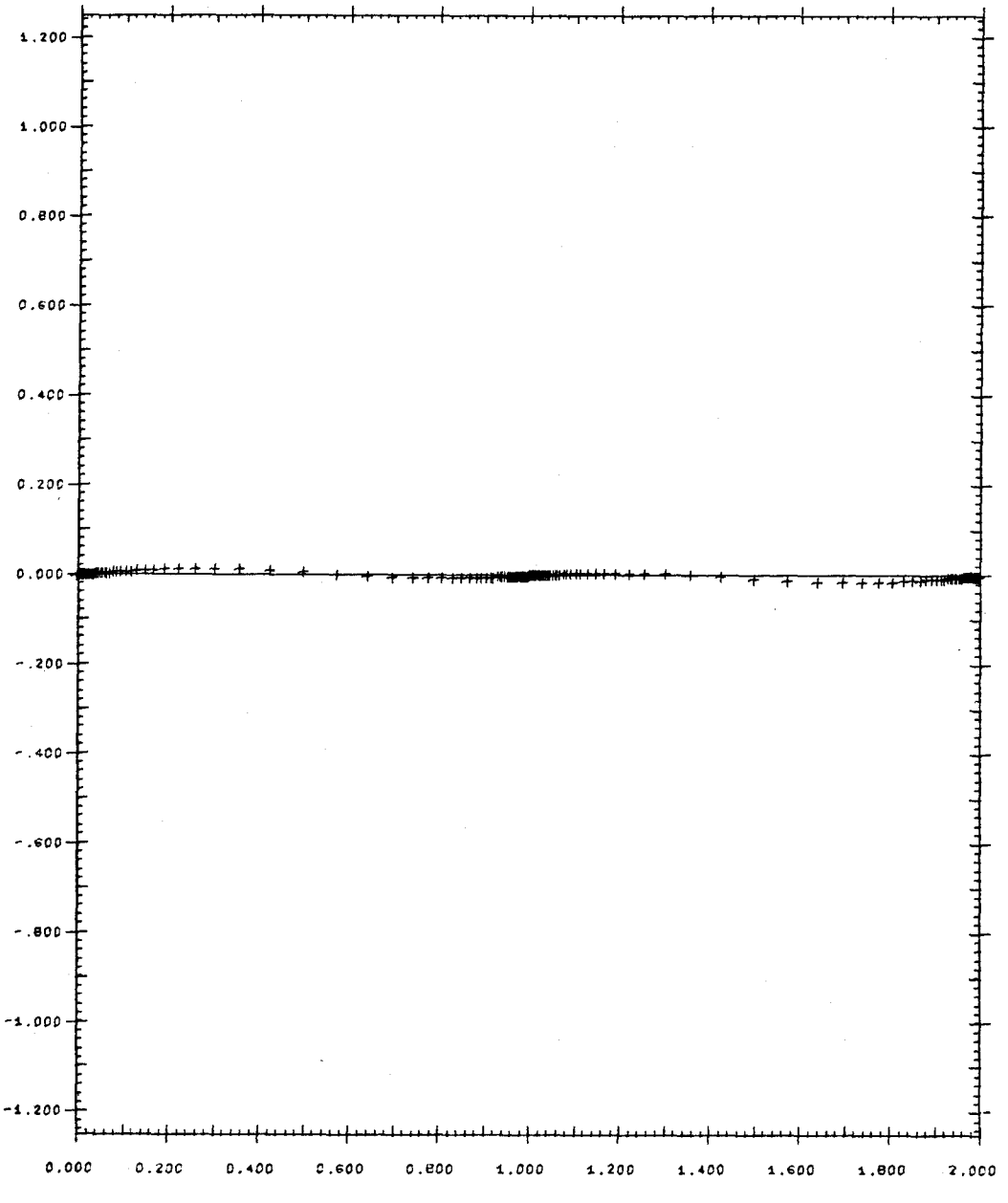

Fig. 5a The evolution of the material interface. Crosses are non-diffusive markers. Roll up and pairing. $\alpha_1 = 0.43$; $\alpha_2 = 0.215$. $R_e = 100$; $\tau = 0$

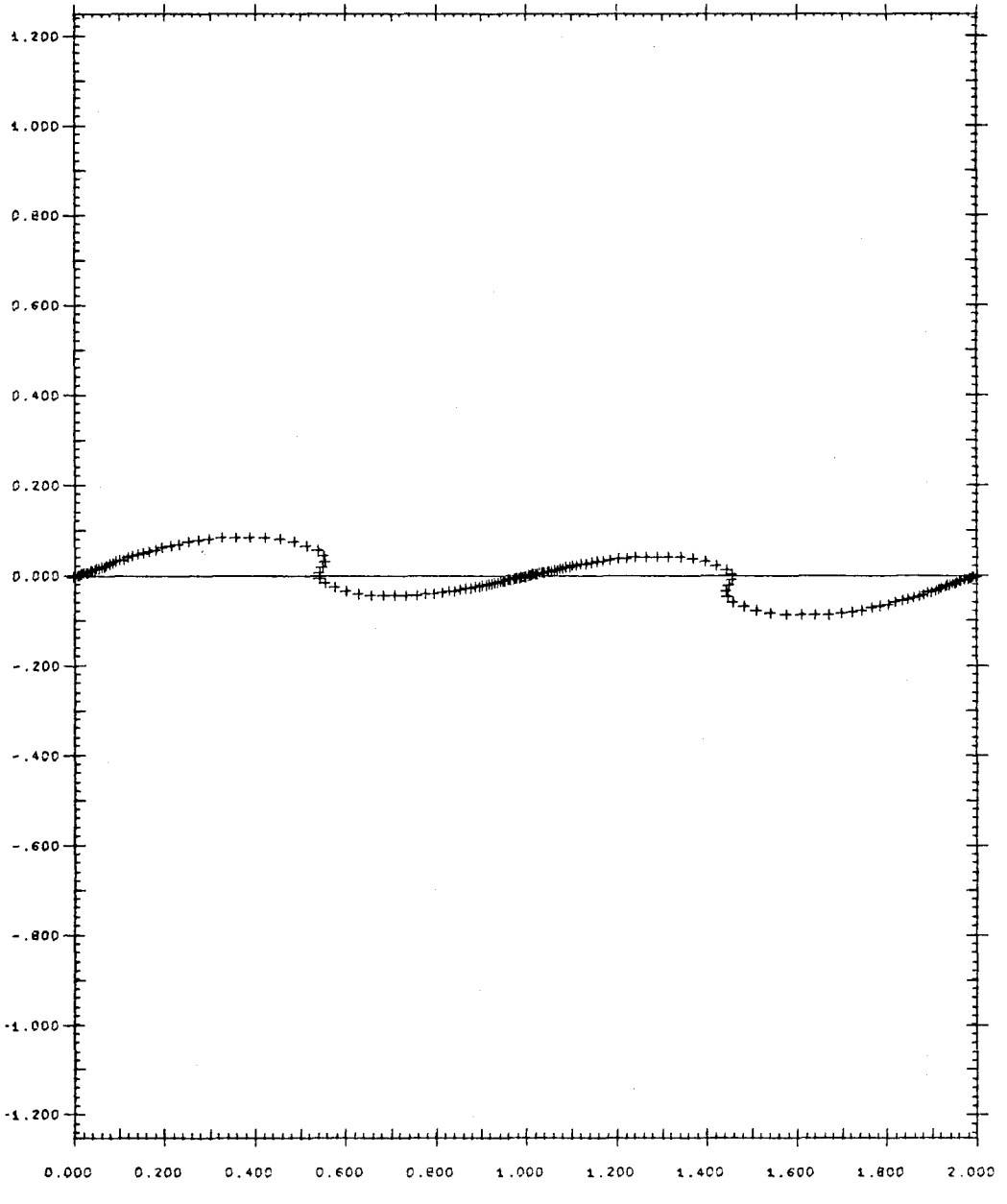

Fig. 5b Same as 5a; $\tau = 0.75$

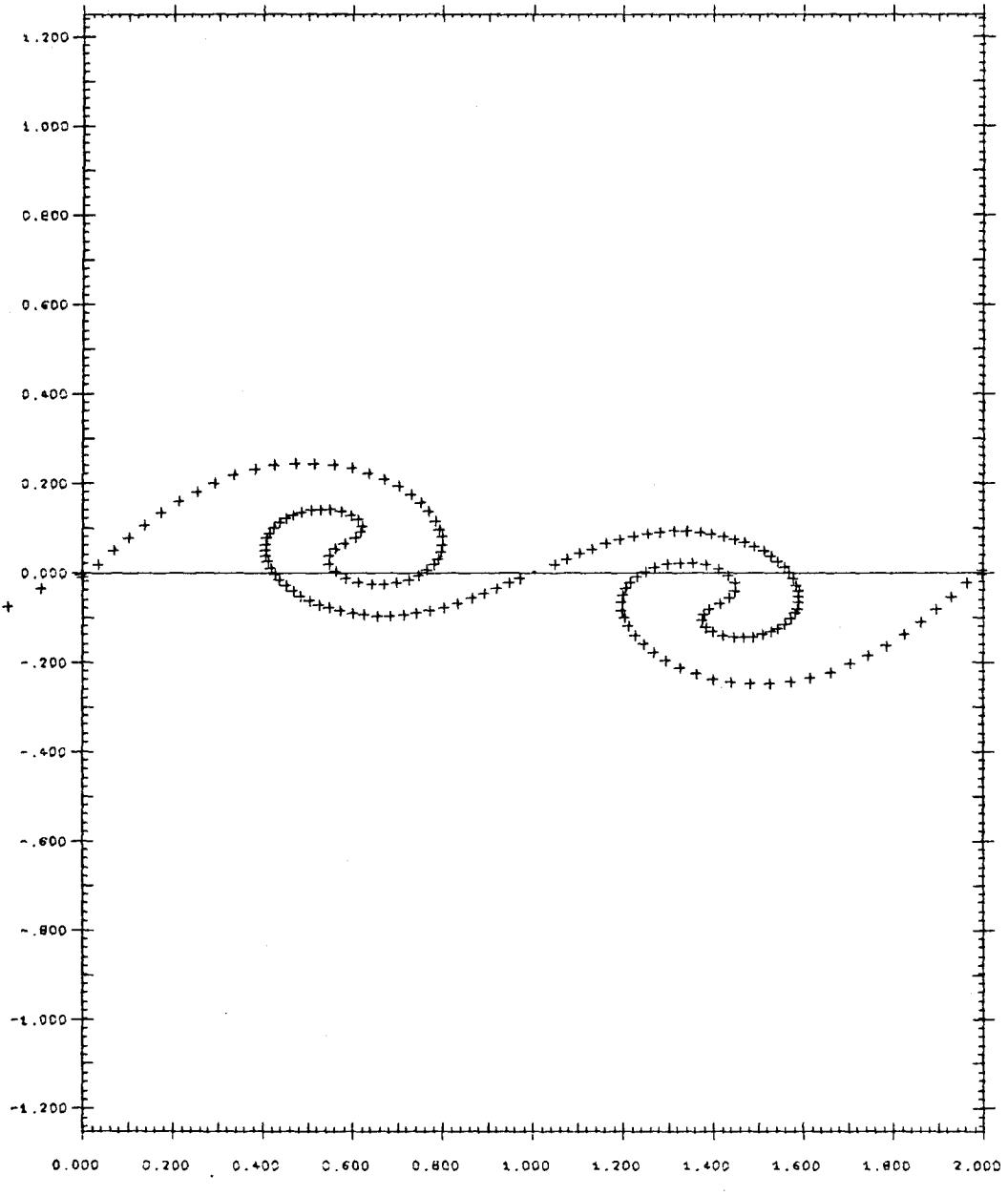

Fig. 5c Same as 5a; τ = 1.50

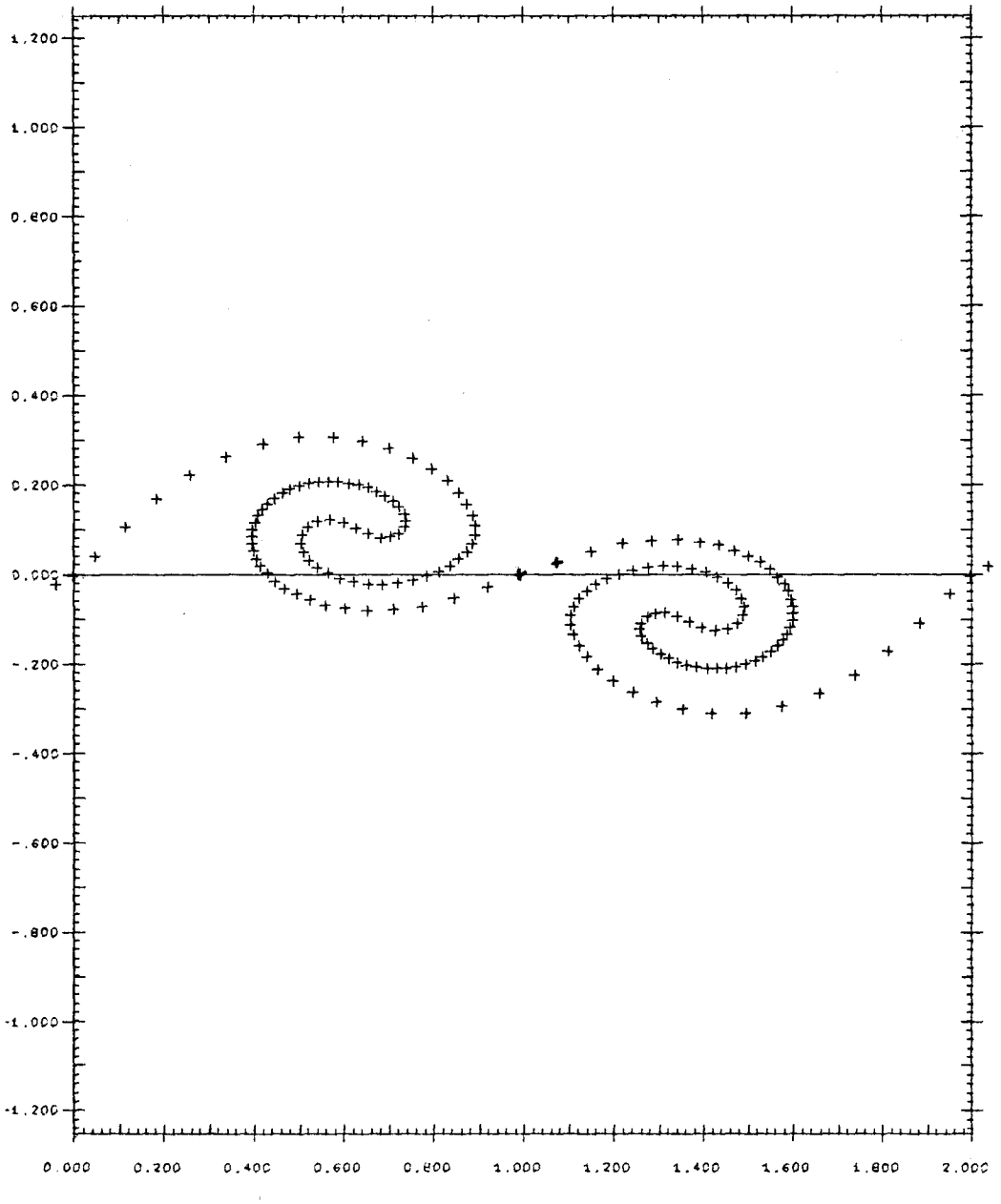

Fig. 5d Same as 5a; $\tau = 1.75$

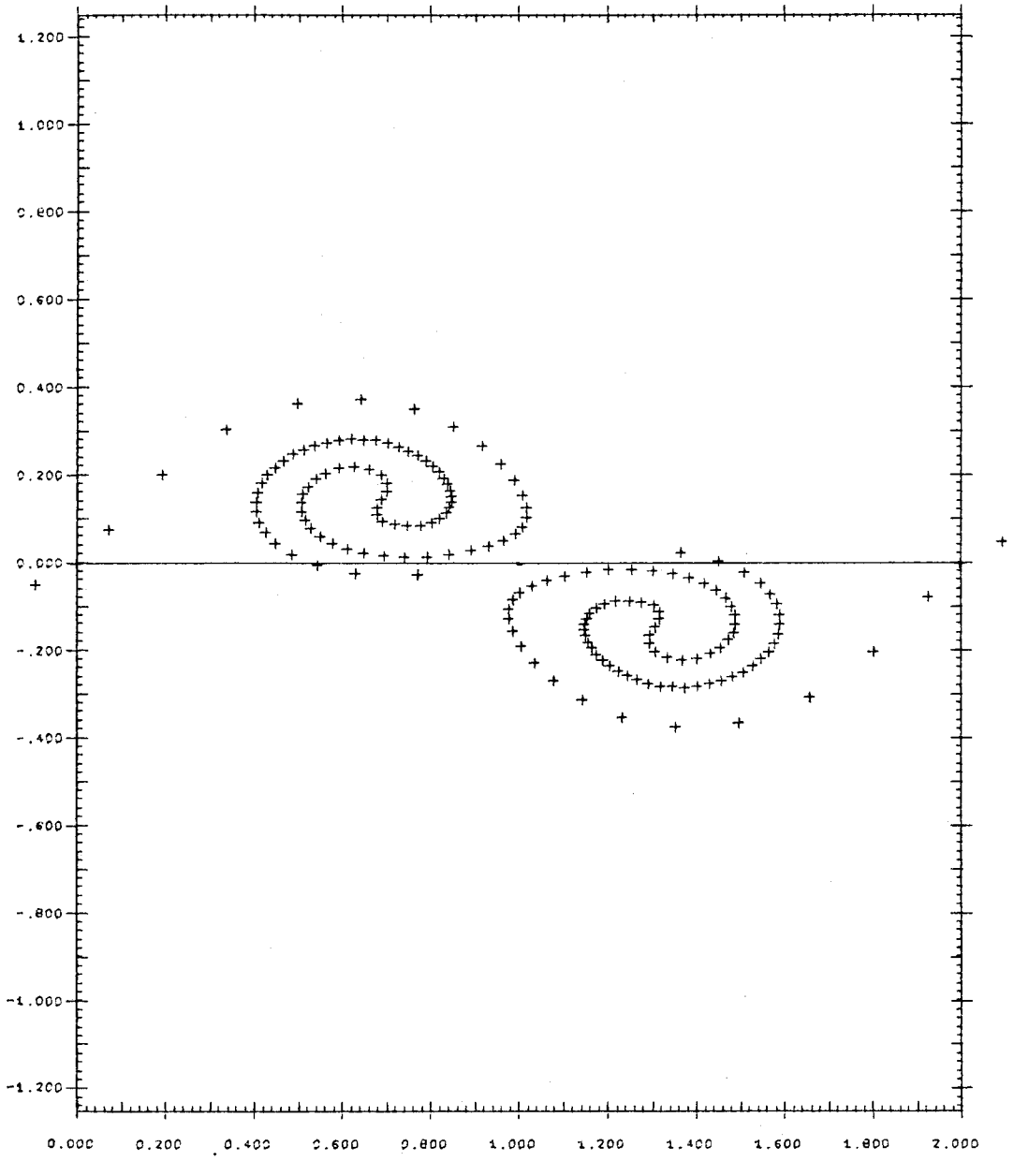

Fig. 5e Same as 5a; τ = 2.00

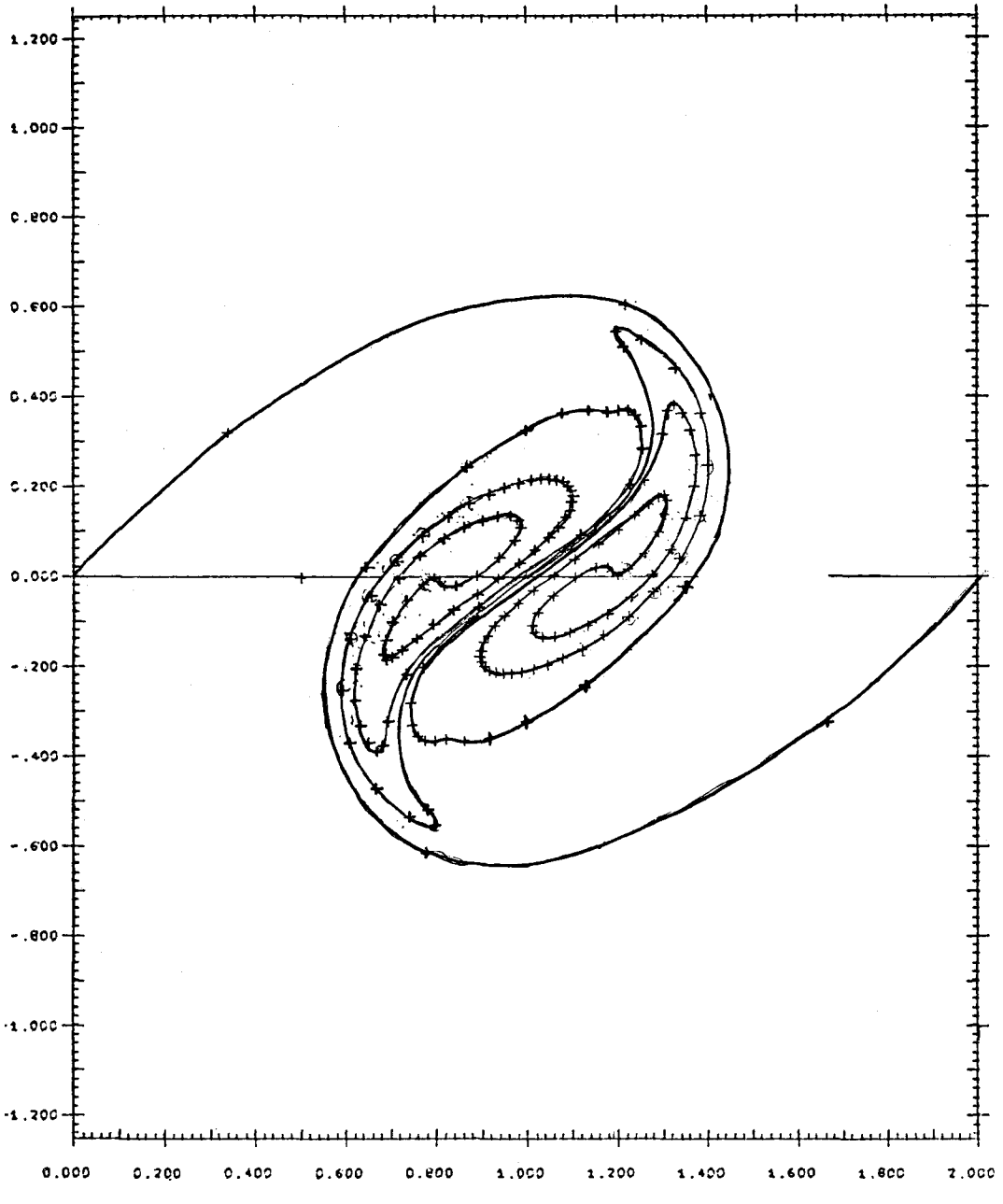

Fig. 5f Same as 5a; $\tau = 3.0$

SINGLE ROLL-UP

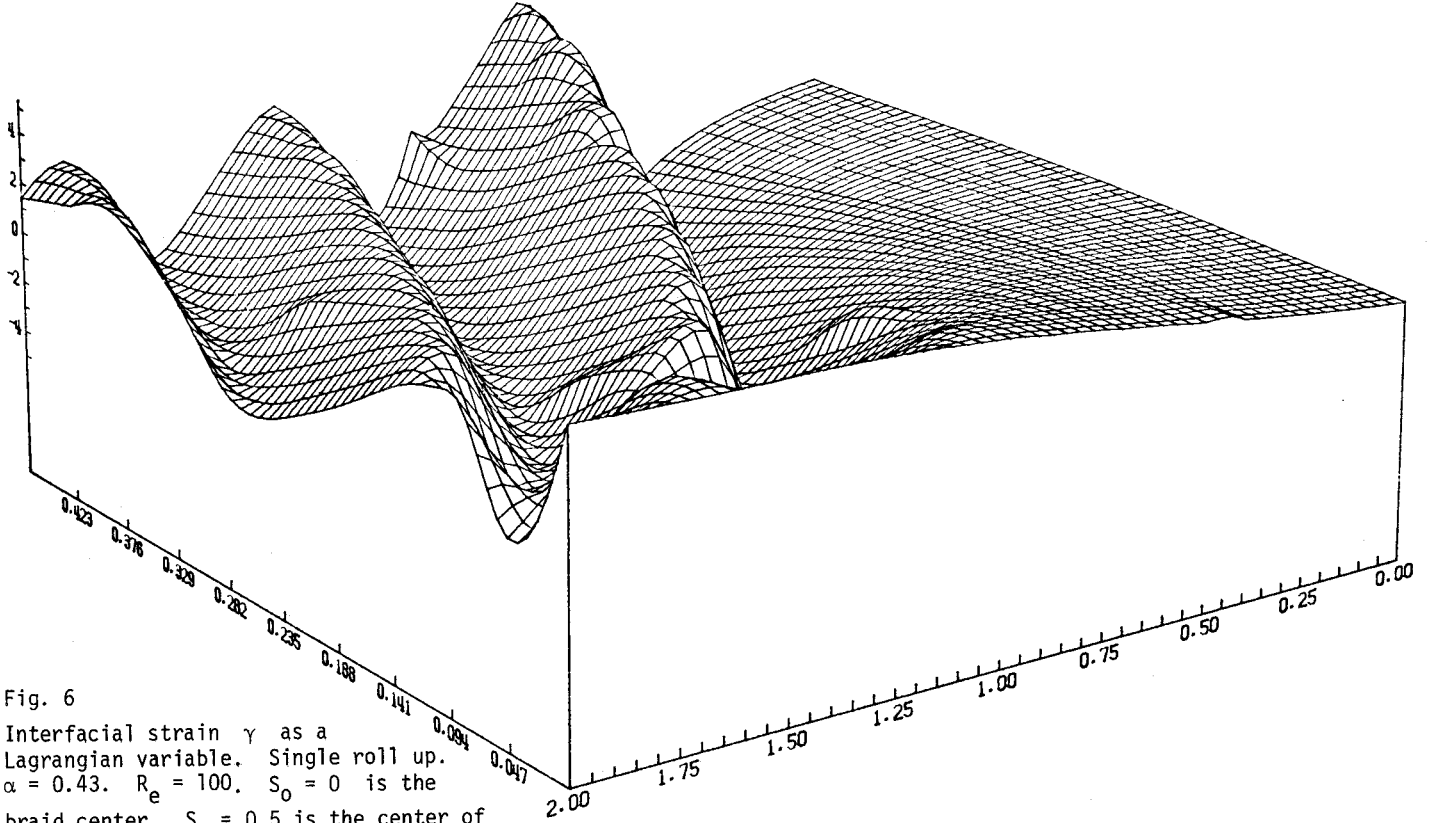

Fig. 6

Interfacial strain γ as a Lagrangian variable. Single roll up. $\alpha = 0.43$. $R_e = 100$. $S_o = 0$ is the braid center. $S_o = 0.5$ is the center of the Vortex core.

RØLL UP AND PAIRING

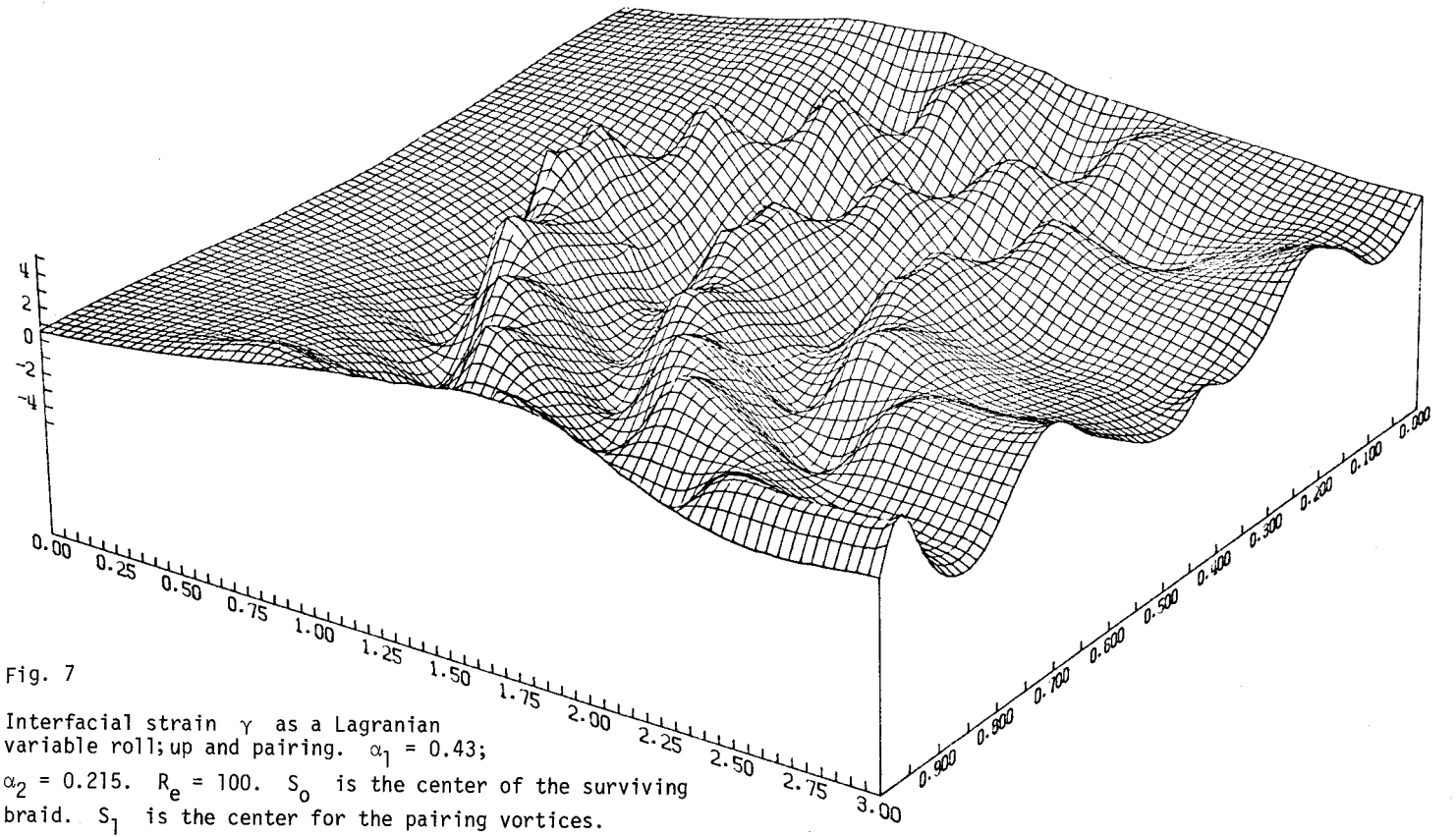

Fig. 7

Interfacial strain γ as a Lagranian variable roll; up and pairing. $\alpha_1 = 0.43$; $\alpha_2 = 0.215$. $R_e = 100$. S_o is the center of the surviving braid. S_1 is the center for the pairing vortices.